



ChemComm

**Metallurgical approach to enhance electrochemical activity  
of magnesium anodes for magnesium rechargeable  
batteries**

Journal:	<i>ChemComm</i>
Manuscript ID	CC-COM-08-2020-005373.R1
Article Type:	Communication

SCHOLARONE™  
Manuscripts

## COMMUNICATION

## Metallurgical approach to enhance electrochemical activity of magnesium anodes for magnesium rechargeable batteries†

Toshihiko Mandai,<sup>\*a</sup> and Hidetoshi Somekawa<sup>b</sup>Received 00th August 2020,  
Accepted 00th month 2020

DOI: 10.1039/x0xx00000x

**A novel metallurgical approach was adopted to enhance the electrochemical activity of Mg anodes for magnesium rechargeable batteries. The primary electrochemical processes were considered to be grain boundary-mediated. Therefore, appropriate control of the grain size combined with Ca alloying of the Mg anode resulted in a remarkable electrochemical Mg<sup>2+</sup>/Mg<sup>0</sup> cycling activity.**

The significant progress in large-scale mobile electric applications and recently accelerated environmental and natural resources issues require highly efficient and environmentally benign electrochemical energy storage systems with enhanced safety and scalability. Post lithium-ion batteries (LiBs) are a series of batteries that mostly incorporate high capacity metallic anodes, such as lithium, magnesium, calcium, and aluminium, combined with high capacity cathode active materials. Magnesium rechargeable batteries (MRBs) are one promising option to fulfil the demands of electrical energy storage while utilizing common chemical resources.<sup>1</sup> The energy density of MRBs can reach 500 Wh kg<sup>-1</sup>, which is twice as much as that of present LiBs. The cost-effectiveness of base Mg metal, due to its large natural abundance, is also favourable for the mass production of large-scale batteries.

There has been significant progress in the research and development of new electrode materials and electrolytes for MRBs, especially in the last several years. Cathode active materials have been discovered that can achieve energy densities of 300 Wh kg<sup>-1</sup> and greater.<sup>2</sup> Highly efficient halogen-free electrolytes that are less-corrosive and compatible with Mg metal have also been developed.<sup>3</sup> In stark contrast to the significant progress in cathode active materials and electrolytes, the development of Mg anodes is still in the early stage due to relatively less research interest. In particular, there have been

only a few reports on strategies adopted to develop Mg metal anodes though systematic research on both materials development and achieving a fundamental understanding of the electrochemical properties of Mg-ion hosts, such as alloys and carbon-based compounds.<sup>4</sup> Group IIIA, IVA, and VA elements are potential candidates for conversion (alloying) anodes of MRBs. Bi and Sn can deliver theoretical specific capacities of ca. 400-600 mAh g<sup>-1</sup> at a redox potential of ca. 0.3 V vs. Mg<sup>2+</sup>/Mg<sup>0</sup>. The thermodynamically lower migration barrier of Mg<sub>3</sub>Bi<sub>2</sub> phase is responsible for its rate capability and cycling stability. The intercalation of Mg ions accompanied with solvated solvents (co-intercalation) was confirmed for certain graphite anodes cycled in conventional ethereal electrolytes. Such host materials that are not based on Mg<sup>2+</sup>/Mg<sup>0</sup> chemistry allow problems associated with the use of Mg metal to be avoided; however, they also cause a loss of the competitive advantages of MRBs over the present LiBs. An artificial interlayer would thus seem to be a possible approach toward the reversible electrochemical cycling of Mg metal anodes.<sup>5</sup> The accommodation of Mg in a magnesiophilic carbon nanosubstrate is also one strategy to improve the electrochemical performance of Mg metal anodes.<sup>6</sup> However, such interfacial manipulation generally requires pre-cycling or pre-deposition of Mg prior to utilization of the anode in a battery. To the best of our knowledge, a metallurgical approach has never been adopted for the development of Mg metal anodes. Both the mechanical properties and physical characteristics of Mg metal have been studied intensively to date in the structural materials field. The microstructural factors of Mg metals and alloys predominantly determine their physical and mechanical properties;<sup>7</sup> therefore, the electrochemical properties could also be modified by metallurgical manipulation. Herein we report the effect of the metallurgical features on the electrochemical properties of Mg metal anodes with respect to the crystal orientation, grain size and alloying, i.e., solid solution element alloying.

<sup>a</sup> Center for Research on Energy and Environmental Materials, National Institute for Materials Science, 1-1 Namiki, Ibaraki, 305-0044 Japan.

<sup>b</sup> Research Center for Structural Materials, National Institute for Materials Science, 1-2-1 Sengen, Ibaraki, 305-0047 Japan.

†Electronic Supplementary Information (ESI) available: Experimental and complete STEM, EBSD, and electrochemistry data. See DOI: 10.1039/x0xx00000x

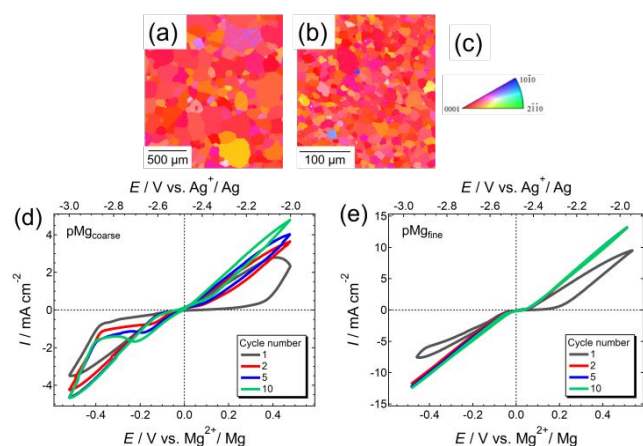


Figure 1. (a, b) EBSD mapping; (c) a color indicator for mirror indices; (d, e) cyclic voltammograms (CVs) of  $\text{pMg}_{\text{coarse}}$  and  $\text{pMg}_{\text{fine}}$ . CVs of each  $\text{pMg}$  electrode were recorded in  $0.3 \text{ mol dm}^{-3} \text{ Mg}[\text{B}(\text{HFIP})_4]_2/\text{G2}$  at  $30^\circ \text{C}$  with a scan rate of  $10 \text{ mV s}^{-1}$ .

As a preliminary survey, the dissolution/deposition ( $\text{Mg}^{2+}/\text{Mg}^0$ ) behaviour of single crystal Mg, oriented (0001) or (10 $\bar{1}$ 0) planes, was examined using cyclic voltammetry (CV). The crystal orientation had a dominant impact on the activity, and the (0001) plane crystal exhibited favourable properties (Fig. S1, ESI $^\dagger$ ). The greater specific electrical conductivity of the (0001) direction than that of the (10 $\bar{1}$ 0) direction is a likely reason for this.<sup>8</sup> The relationship between microstructural factors (texture) and electrochemical activity was further investigated using pure Mg metal ( $\text{pMg}$ ) with different grain sizes. The  $\text{pMg}$  (commercial purity of 99.96 wt%) produced by extrusion was subjected to electrochemical tests. Heat treatments of extruded  $\text{pMg}$  at different temperature were subsequently adopted, and this treatment enabled the successful control of the grain size. As evidenced by electron backscattered diffraction (EBSD) mapping (Fig. 1), one  $\text{pMg}$  sample consisted mainly of fine grains ( $\text{pMg}_{\text{fine}}$ ) with an average grain size of  $<20 \mu\text{m}$ , while another sample consisted of both fine and relatively coarse ( $>100 \mu\text{m}$ ) grains ( $\text{pMg}_{\text{coarse}}$ ). The crystal orientation in

both  $\text{pMg}$  samples was almost uniform, preferentially accumulated to the (0001) direction, irrespective of the grain size. Primary electrochemical studies on the  $\text{pMg}$  samples with different grain sizes revealed favourable electrochemical activity for  $\text{pMg}_{\text{fine}}$  rather than  $\text{pMg}_{\text{coarse}}$  because surface activation was accomplished by only one  $\text{Mg}^{2+}/\text{Mg}^0$  cycle for the former  $\text{pMg}$  (Fig. 1). Subsequent cycles further corroborated the superior electrochemical performance of  $\text{pMg}_{\text{fine}}$  over  $\text{pMg}_{\text{coarse}}$ , especially in the deposition process. A commercial  $\text{pMg}$  ribbon that consisted of a mixture of fine and coarse grains also showed relatively less electrochemical activity (Fig. S2, ESI $^\dagger$ ). The grain boundary-less single crystal samples showed smaller current density for the magnesium  $\text{Mg}^{2+}/\text{Mg}^0$  cycle processes by one order of magnitude (Fig. S1, ESI $^\dagger$ ). These results strongly imply that the grain boundaries mediate the primary electrochemical processes. The free energy of grain boundaries or defects is known to determine the electronic properties of agglomerated particles in polycrystalline compounds.<sup>9</sup> The electrochemical activity of Mg anodes could thus be controlled by perturbation of the free energy of the grain boundaries through alloying.

Fig. 2 shows EBSD maps of a series of Mg-X anodes. Non-rare earth elements that are more than 0.3 at% soluble in Mg were selected as the solute element X. Despite the presence of different elements, the grain size of Mg in Mg-X was well controlled to less than  $20 \mu\text{m}$  via extrusion and subsequent heat treatments. Solute element doping also has a minor impact on the crystal orientation, although the accumulation of the (0001) direction was well preserved, irrespective of the choice of alloying element. Contrary to these overall texture characteristics, the segregation behaviour was alloying element-dependent. High-angle annular dark-field scanning

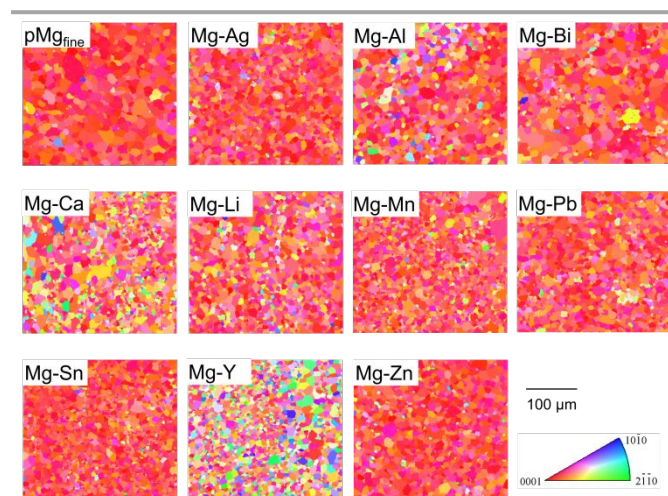


Figure 2. EBSD maps of the Mg-X. A color indicator for mirror indices is also shown.

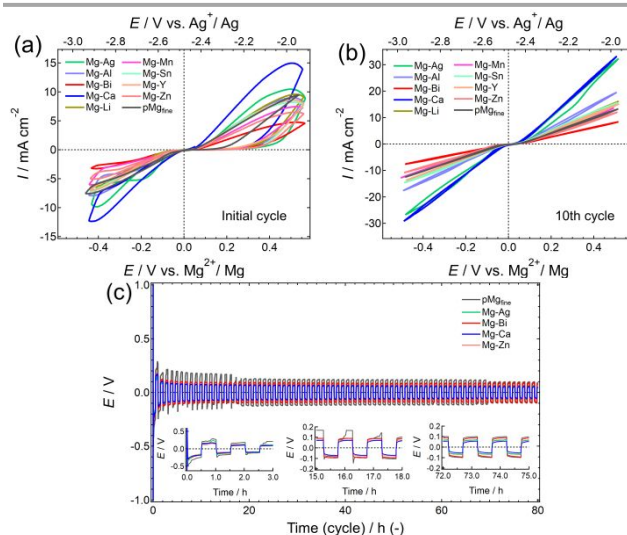


Figure 3. (a) Initial and (b) 10 $^{\text{th}}$  cycle CV curves, and (c) galvanostatic magnesium dissolution/deposition ( $\text{Mg}^{2+}/\text{Mg}^0$ ) cycling behaviour of  $\text{pMg}_{\text{fine}}$  and selected Mg-X cycled in  $0.3 \text{ mol dm}^{-3} \text{ Mg}[\text{B}(\text{HFIP})_4]_2/\text{G2}$  at  $30^\circ \text{C}$ . CV measurements were conducted using a three-electrode cell, where  $\text{pMg}$  or Mg-X, Pt coil, and  $\text{Ag}^+/\text{Ag}$  were served as working, counter, and reference electrodes, respectively. For galvanostatic cycling tests, two-electrode symmetric cells were fabricated and a current density of  $0.5 \text{ mA cm}^{-2}$  was applied for each  $\text{Mg}^{2+}/\text{Mg}^0$  process.

transmission electron microscopy (HAADF-STEM) images indicate the segregation and dispersion of the precipitate particles in the entire texture distribution for the Mg-X anodes, with the exceptions of Mg-Al and Mg-Zn (Fig. S3, ESI<sup>†</sup>). For Mg-Al and Mg-Zn, Al and Zn nanocrystals were segregated preferentially at the Mg grain boundaries. However, STEM observations of Mg-rare earth alloys suggests the segregation of alloying elements occurs preferentially at the grain boundaries.<sup>10</sup> Significant changes in the mechanical properties for alloying with solute elements at 0.3 at%<sup>11</sup> also strongly corroborates segregation at the grain boundaries, although no microstructural evidence could be obtained, likely due to the low alloying levels and the heat treatment conditions.

Solute element alloying has a significant effect on the electrochemical activity. The electrochemical  $\text{Mg}^{2+}/\text{Mg}^0$  activities of a series of Mg-X anodes were evaluated using CV and galvanostatic cycling measurements. CV revealed that the overpotential for the initial Mg dissolution (anodic) process was increased by ca. 100 mV with solute element alloying (Fig. 3a and Table S1, ESI<sup>†</sup>). In contrast to the initial dissolution process, decreased overpotentials for deposition were observed for Mg-Ag and Mg-Ca in the reverse cathodic scan (Fig. 3a). Mg-Bi and Mg-Zn required large overpotentials for Mg dissolution. This dependence of the electrochemical behaviour on the alloying element was further emphasized in subsequent cycles. At the 10th cycle, the overpotential for  $\text{Mg}^{2+}/\text{Mg}^0$ , defined as the potential where a current density of  $\pm 0.1 \text{ mA cm}^{-2}$  was observed, was in the order of Mg-Ca < Mg-Ag <  $\text{pMg}_{\text{fine}}$   $\approx$  Mg-Al  $\approx$  Mg-Li  $\approx$  Mg-Mn  $\approx$  Mg-Sn  $\approx$  Mg-Y < Mg-Zn < Mg-Bi. A similar trend was also observed in a typical Grignard reagent (Fig. S4, ESI<sup>†</sup>). It has been reported that the surface of Mg metal is utilized inhomogeneously during deposition/dissolution cycling.<sup>12</sup> The surface of Mg-X was utilized inhomogeneously as well (Fig. S5, ESI<sup>†</sup>). However, Mg-Ca after cycling showed relatively smooth surface while some decomposition products and micro-particles were observed for Mg-Zn. Such difference in surface behaviour may affect the electrochemical activity. The electrochemical activity of a series of Mg-X anodes was further assessed by galvanostatic  $\text{Mg}^{2+}/\text{Mg}^0$  cycling with symmetric two-electrode assemblies. The extreme cases of Mg-Ag, Mg-Bi, Mg-Ca, Mg-Zn, and  $\text{pMg}_{\text{fine}}$  were investigated here. The overpotentials for the galvanostatic  $\text{Mg}^{2+}/\text{Mg}^0$  processes at  $0.5 \text{ mA cm}^{-2}$  were consistent with the CV cycling results (Fig. 3(c)), while the corresponding Coulombic efficiencies are

comparable, ca. 97-98%, among the studied alloys (Fig. S6, ESI<sup>†</sup>). Mg-Ca showed the lowest overpotential in the series while Mg-Bi and Mg-Zn required relatively larger overpotentials during the overall cycling periods. The detailed reasons and mechanisms for such solute-dependent activities are still unclear; however, the chemical and physical characteristics of the solute elements can induce the observed differences. For example, the standard electrode potential of Ca ( $-2.76 \text{ V vs. SHE}$ ) implies a relatively reductive nature ( $-2.36 \text{ V vs. SHE}$  for Mg). Ca can thus be dissolved easily during the initial anodic scan and the resulting defects can function as active sites. The relatively large lattice mismatch of Ca against Mg also causes large lattice strain in the vicinity of grain boundaries.<sup>7</sup> Such physical strain can contribute to an acceleration of intergranular fracture, which can also lead to defect formation in Mg-Ca anodes. Intrinsically hindered Bi oxidation and small lattice mismatch between Mg and Zn would cause the lower electrochemical activities of Mg-Bi and Mg-Zn. On the other hand, the electron orbitals hybridization between Mg and Ag atoms and consequent binding characteristics are assumed to impart enhanced electrochemical activity of the Mg-Ag alloy.<sup>13</sup>

The energy density of MRBs can be improved by the solute element doping of Mg anodes. Enhanced discharge capacities of a typical MRB with a  $\text{MgMn}_2\text{O}_4$  cathode were achieved using Mg-Ca as an anode (Fig. 4 and Fig. S7, ESI<sup>†</sup>). Although there was little improvement in the magnitude of the energy density, this approach opens the possibility of practical MRBs with favourable electrochemical performance by the simple solute element alloying of Mg anodes.

In summary, the enhancement of electrochemical properties of Mg anodes was demonstrated by appropriate control of the crystal orientation and grain sizes associated with alloying. There is a strong correlation of the electrochemical  $\text{Mg}^{2+}/\text{Mg}^0$  processes with the grain boundary characteristics. This novel approach is particularly effective for the fabrication of high-performance MRBs without complicated preliminary processes and/or specific cell formulations. We consider that this strategy will open the door to the design of new MRBs. Further interfacial and numerical studies are necessary to understand the characteristics of Mg-X in depth and to achieve optimized anodes with respect to their micro/nanostructures.

## Conflicts of interest

There are no conflicts to declare.

## Notes and references

- 1 J. Muldoon, C. B. Bucur and T. Gregory, *Chem. Rev.*, 2014, **114**, 11683; Z. Ma, D. R. MacFarlane and M. Kar, *Batteries & Supercap*, 2019, **2**, 115.
- 2 M. Mao, T. Gao, S. Hou, F. Wang, J. Chen, Z. Wei, X. Fan, X. Ji, J. Ma and C. Wang, *Nano Lett.*, 2019, **19**, 6665.
- 3 J. T. Herb, C. A. N.-Lund and C. B. Arnold, *ACS Energy Lett.*, 2016, **1**, 1227; Z. Z.-Karger, M. E. G. Bardaji, O. Fuhr and M. Fichtner, *J. Mater. Chem. A*, 2017, **5**, 10815.
- 4 J. Niu, Z. Zhang and D. Aurbach, *Adv. Energy Mater.*, 2020, **10**, 2000697; S. C. Jung and Y.-K. Han, *J. Phys. Chem. C*, 2018, **122**,

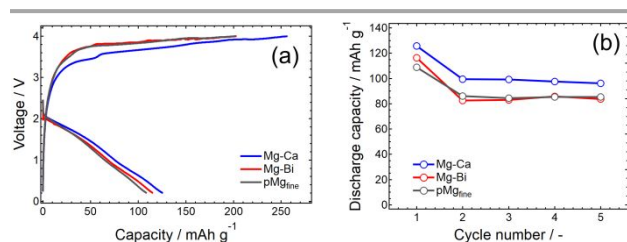


Figure 4. (a) Initial charge-discharge profiles and (b) discharge capacities of the  $[\text{Mg-X}]0.3 \text{ mol dm}^{-3} \text{ Mg}[\text{B}(\text{HFIP})_4]_2/\text{G2}[\text{MgMn}_2\text{O}_4]$  cells. A current density of  $10.4 \text{ mA g}^{-1}$  (1/25 C-rate based on the mass of  $\text{MgMn}_2\text{O}_4$ ) was applied at  $30 \text{ }^\circ\text{C}$ . Cut-off:  $+4.0$ – $+0.2 \text{ V}$ .

- 17643; D.-M. Kim, S. C. Jung, S. Ha, Y. Kim, Y. Park, J. H. Ryu, Y.-K. Han and K. T. Lee, *Chem. Mater.*, 2018, **30**, 3199.
- 5 S.-B. Son, T. Gao, S. T. harvey, K. X. Steirer, A. Stokes, A. Norman, C. Wang, A. Cresce, K. Xu and C. Ban, *Nat. Chem.*, 2018, **10**, 532; K. Tang, A. Du, S. Dong, Z. Cui, X. Liu, C. Lu, J. Zhao, X. Zhou and G. Cui, *Adv. Mater.*, 2020, **32**, 1904987.
- 6 H.-D. Lim, D. H. Kim, S. Park, M. E. Lee, H.-J. Jin, S. Yu, S. H. Oh and Y. S. Yun, *ACS Appl. Mater. Interfaces*, 2019, **11**, 38754.
- 7 H. Somekawa, *Mater. Trans.*, 2020, **61**, 1.
- 8 P. W. Bridgman, *Proc. Am. Acad. Arts Sci.*, 1932, **67**, 29.
- 9 S.-D. Mo, W. Y. Ching, M. F. Chisholm and G. Duscher, *Phys. Rev. B*, 1999, **60**, 2416.
- 10 J. P. Hadorn, K. Hantzsche, S. Yi, J. Bohlen, D. Letzig, J. A. Wollmershauser and S. R. Agnew, *Metall. Mater. Trans. A*, 2012, **43A**, 1347.
- 11 H. Somekawa, A. Singh, T. Mukai, T. Inoue, *Philo. Mag.*, 2016, **96**, 2674.
- 12 T. Mandai, *ACS Appl. Mater. Interfaces*, 2020, **12**, 39135.
- 13 H. Somekawa, T. Tsuru, *Scr. Mater.*, 2017, **130**, 114.